Received: 27 February 2024 | Revised: 18 June 2024 | Accepted: 19 June 2024

DOI: 10.1002/ppp3.10554

RESEARCH ARTICLE

Plants People Planet PPP Open Access

Solar arrays create novel environments that uniquely alter plant responses

Matthew A. Sturchio[1] | Steven A. Kannenberg[1,2] | Tillie A. Pinkowitz[1] | Alan K. Knapp[1]

[1]Department of Biology and Graduate Degree Program in Ecology, Colorado State University, Fort Collins, Colorado, USA

[2]Department of Biology, West Virginia University, Morgantown, West Virginia, USA

Correspondence
Matthew A. Sturchio, Department of Biology and Graduate Degree Program in Ecology, Colorado State University, Fort Collins, CO 80523, USA.
Email: matthew.sturchio@colostate.edu

Funding information
Department of Agriculture; National Institute of Food and Agriculture, Grant/Award Number: 2021-68012-35898; University of Illinois, Grant/Award Numbers: 2021-68012-35898, 2021–2025; Colorado State University

Societal Impact Statement

Globally, the combustion of fossil fuels represents the vast majority of greenhouse gas emissions, and as such, a transition to renewable forms of energy provides the greatest potential for mitigating climate warming. Although solar photovoltaic energy generation is a leading climate solution, these energy facilities have a significant spatial footprint. Naturally, concerns regarding the coexistence of solar development in agriculturally productive and pristine native ecosystems remain. This study offers insight for how plants respond to novel environmental conditions within a solar array and contextualizes results to inform future array siting, design, and management to realize a sustainable solar energy future.

Summary

- Photovoltaic (PV) solar arrays impose dynamic shading regimes and redistribute precipitation to the ecosystems beneath, leading to spatial and temporal heterogeneity in plant growth environments. Although PV are known to alter ecosystem-level processes in managed and native landscapes, the control of PV-induced microenvironments on plant ecophysiological responses are largely unexplored. A more robust and mechanistic understanding of how PV microenvironments control plant response will inform management of existing solar arrays and provide insight for future arrays designed to enhance ecosystem services.
- Here, we evaluated carbon (photosynthetic parameters) and water relations (daily patterns of leaf water potential (ψ_L) and stomatal conductance (g_{sw})) in a C_3 perennial grass (*Bromus inermis*) across PV microsites within a 1.6 ha (1.2 MW) array in semiarid Colorado, USA.
- Light-saturated photosynthetic rate was surprisingly consistent spatially, not differing between plants growing in near full sun (between PV rows) versus those growing in shadier microsites beneath panels (~28% of full sunlight). Additionally, plants located in microsites receiving only direct sunlight in the morning, when air temperature and vapor pressure deficits (VPD) were low, had greater ψ_L and g_{sw} than plants receiving direct sunlight primarily in the hotter drier afternoon.

This is an open access article under the terms of the Creative Commons Attribution License, which permits use, distribution and reproduction in any medium, provided the original work is properly cited.
© 2024 The Author(s). *Plants, People, Planet* published by John Wiley & Sons Ltd on behalf of New Phytologist Foundation.

- Thus, while soil moisture is a primary control of plant productivity in most water-limited grasslands, we found that VPD was a better predictor of daily patterns of leaf-level photosynthetic and water relations responses that control aboveground biomass production in a PV array. These findings provide new mechanistic insight for evaluating vegetation management strategies in semiarid PV arrays.

KEYWORDS
agrivoltaics, diurnal physiology, ecophysiology, ecovoltaics, renewable energy ecology, solar land use

1 | INTRODUCTION

As the cost of photovoltaic (PV) energy decreases (Feldman et al., 2021), the deployment of ground mounted PV arrays is expected to expand, covering up to ~61,000 km^2 in the United States by 2050 (Larson, 2020). As a result, an understanding of the potential impacts of PV infrastructure on ecosystems is needed to inform more sustainable array design, siting, and management (Hernandez et al., 2019; Sturchio & Knapp, 2023). A well-documented consequence of PV infrastructure is the novel patterns of environmental heterogeneity (e.g., light, temperature, and water) induced by the physical presence of rows of PV panels suspended above the ecosystems beneath (Adeh et al., 2018; Armstrong et al., 2016; Choi et al., 2020; Choi et al., 2023; Sturchio et al., 2022; Sturchio & Knapp, 2023; Tanner et al., 2020). Indeed, PV-induced modifications in light and water environments have been linked to altered patterns of aboveground net primary production (ANPP) in a wide range of ecosystems globally (Adeh et al., 2018; Andrew et al., 2021; Armstrong et al., 2016; Bai et al., 2022; Kannenberg et al., 2023; Sturchio et al., 2022; Sturchio et al., 2024; Sturchio & Knapp, 2023; Zhang et al., 2024). Less well-known are the underlying ecophysiological responses of plants to alterations in light and water availability generated by PV arrays. Such responses have the potential to provide unique mechanistic insight for understanding plant growth patterns within PV arrays.

Currently, our understanding of plant responses to different microenvironments within PV arrays are limited to short-term measurements of desert species (Hernandez et al., 2020; Smith et al., 1987; Tanner et al., 2021; Wynne-Sison et al., 2023), as well as seasonal and daily ecophysiological responses of irrigated specialty crops (Barron-Gafford et al., 2019; Juillion et al., 2022; Marrou et al., 2013) in agrivoltaic (AV) settings (an approach to solar energy development where the land beneath PV panels is co-utilized for agricultural production, Dupraz et al., 2011, Dinesh & Pearce, 2016). However, the majority of AV land use to date involves perennial agroecosystems, such as restored and managed grasslands, generating ecosystem services in the form of forage production and pollinator habitat (Inspire AV Map). How these long-lived perennial species will respond to the novel environments imposed by PV arrays is unresolved.

Environmental variation in light, temperature, and water are well-known to affect plant physiology at the leaf, whole-plant, and ecosystem levels (Atkin & Tjoelker, 2003; Cabon et al., 2022; Ellsworth & Reich, 1992; Smith & Dukes, 2013; Wright et al., 2004). For example, the dichotomy of sun and shade leaf photosynthetic response has been well-documented in many natural ecosystems (Givnish, 1988; Hamerlynck & Knapp, 1994; Pearcy & Sims, 1994), but a growing body of literature in PV arrays has demonstrated that plants may benefit from reduced exposure to direct sunlight in arid and semi-arid climates (Barron-Gafford et al., 2019; Kannenberg et al., 2023; Knapp & Smith, 1990; Sturchio et al., 2024). Furthermore, dynamic light regimes and the redistribution of precipitation (via panel runoff) result in spatially heterogeneous patterns of soil moisture (SM) that have been shown to weaken (Sturchio et al., 2022) the otherwise robust positive relationship between SM and ANPP in semiarid grasslands (Knapp et al., 2002; La Pierre et al., 2016; Post & Knapp, 2021; Sala et al., 1988). A proposed explanation for this disruption is that because microsites within PV arrays can vary dramatically in both the amount of sunlight received and the daily timing of when direct sunlight is incident, the altered solar radiation regime dampens SM as a driver of plant growth. Ecophysiological evidence consistent with this hypothesis and supporting these patterns of ANPP is lacking, however.

Here, we assessed the physiological response of a C_3 perennial grass to PV-induced environmental heterogeneity in a formerly managed semiarid grassland in Colorado, USA. Past research at this site revealed consistent and substantial variation in ANPP depending on the microsite within the PV array (see Sturchio et al., 2022; Sturchio et al., 2024). The goals of this study were to (1) quantify how environmental heterogeneity within an PV array alters *Bromus inermis* photosynthetic capacity and leaf water relations, (2) determine relationships between daily patterns of stomatal conductance (g_{sw}) and leaf water potential (ψ_L) and key environmental drivers, and finally (3), relate ecophysiological patterns in this dominant grass to aboveground productivity.

We expected that (1) the wide variation of spatial and temporal amounts and patterns of light availability within the PV array would lead to daily and seasonal physiological responses that differed dramatically from those outside the array, (2) that within the PV array, plants receiving morning light would strongly differ in their rates of gas exchange (g_{sw}) and overall water relations than plants receiving afternoon light, and (3) that daily patterns of leaf water status and stomatal response, which should relate to productivity, will be better

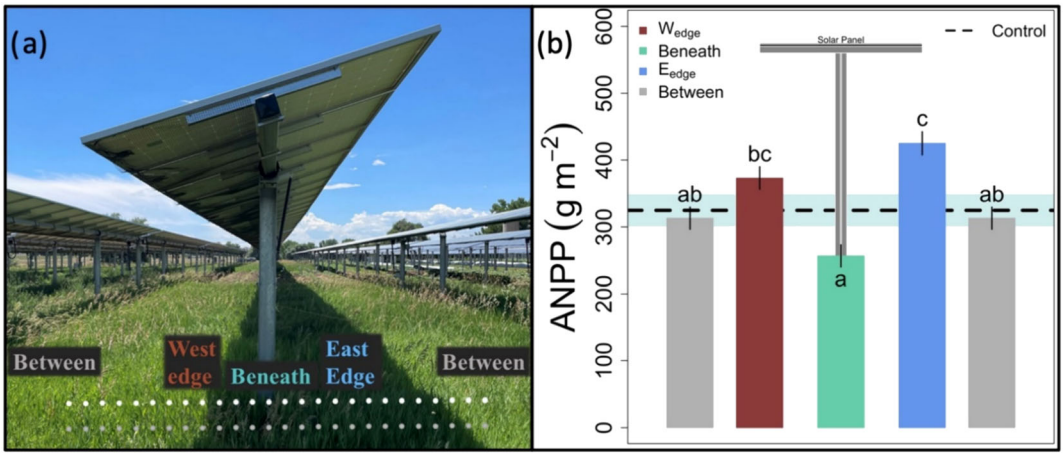


FIGURE 1 (a): Annotated photograph depicting the experimental microsites (between, east edge (E_{edge}), beneath, and west edge (W_{edge})) used for physiological measurements and end of season plant productivity sampling. SM sensor layout (20 cm between sensors, E-W) at two depths is shown using white and gray dots. (b): Spatial patterns of mean ANPP for 2022 for experimental microsites ($n = 12$ for each AV microsite). Patterns of production are comparable to those reported previously at the same site (Sturchio et al., 2022; Sturchio et al., 2024). Lines on vertical bars represent standard error from the mean. Letters above bars denote statistical differences ($p < 0.05$). The control microsite mean ANPP is depicted by a dashed horizontal line ($n = 4$ for control area) with a light blue shadow representing standard error from the mean.

predicted by the atmospheric demand for water (vapor pressure deficit (VPD) as determined by humidity and temperature) during periods of direct sunlight rather than the supply of water to plants (SM).

2 | MATERIALS AND METHODS

Research was conducted at Jack's Solar Garden (JSG), an AV research facility (https://www.jackssolargarden.com/) near Longmont, CO (elevation 1508 m, 40°07′18.9″N 105°07′49.9″W). JSG is on Mountain Daylight Time (UTC—06:00) and all references to time of day are reported on a 24-h clock (00:00–24:00). The climate is cold semiarid (Köppen classification Bsk) with a mean annual temperature of 9.8°C and 367 mm of precipitation annually (Colorado Climate Center http://ccc.atmos.colostate.edu/). Historically, the 1.5 ha site was managed for hay production, but active management (mowing) ended in 2019 when the PV array was installed. Soils at JSG are a clay loam/sandy clay loam (39% clay, 20% silt, 41% sand) with a pH of ~7.45 and bulk density of 1.03 g/cm^3. The grassland at JSG is dominated (>80% cover) by a perennial nonnative C_3 grass (*B. inermis*) with scattered individuals of *Dactylis glomerata* (C_3 Orchard grass), *Medicago sativa* (Alfalfa), and *Tragopogon dubius* (C_3 forb) interspersed. This study took place beneath PV panels mounted 1.8 m above the ground (Figure 1a). Individual PV panels at JSG are 2 m (east–west) × 1 m (north–south) and are mounted in series on a single axis tracking system (tracking east–west, Figure 1a).

We established three 10.4 m transects perpendicular to the rows of PV panels within a portion of JSG that has been maintained as an undisturbed perennial grassland (Figure 1a). Each transect was comprised of four replicate sampling points along the environmental gradient created by the PV panels (*E_{edge}*; beneath eastern edge of panel where rainfall is redistributed, *W_{edge}*; beneath western edge of panel where rainfall is redistributed, *Beneath*; directly beneath panel, in line with the panel support beams, and *Between*; between rows of panels, Figure 1a). Each experimental plot was 1 × 0.5 m with a 3 m north–south gap separating transects. Control plots were located ~20 m outside the solar array in a similarly managed portion of the formerly hayed grassland but not affected by the shade or precipitation redistribution from panels. At the end of the growing season (September 29th), all experimental plots ($n = 52$) were sampled for ANPP (g m^{-2}). Because the site had been mowed at the end of the 2021 growing season, aboveground biomass accumulating in 2022 represented ANPP. While harvesting, biomass was sorted by functional group (grass vs. forb). Harvested biomass was dried at 60°C for 72 h before being weighed to the nearest 0.01 g.

2.1 | Environmental measurements

Air temperature (T_{air}, C°), relative humidity (RH%), and photosynthetic photon flux density (PPFD, μmol m^{-2} s^{-1}), were continuously recorded at a meteorological station on site at JSG, May–September 2022, henceforth referred to as the growing season. We recorded PPFD every 15 min using CS310 Quantum Sensors (Campbell Scientific, Logan, UT) located in plots directly between PV support posts (Figure 1a, Between), 80 cm east of support posts (Figure 1a, E_{edge}), directly in line with support posts (Figure 1a, Beneath), and 80 cm west of support posts (Figure 1a, W_{edge}). E_{edge} and W_{edge} were located 80 cm in either direction of support posts to quantify temporal patterns of light availability underneath eastern and western drip edges, respectively. PPFD measurements were recorded at grass canopy height, which required continuous adjustments as the canopy grew taller throughout the growing season. An on-site meteorological station provided control plot PPFD, T_{air}, and RH%.

Volumetric water content (VWC, referred to as SM in the text) was measured every 15 min for all experimental microsites and control plots using CS616 Soil Moisture Sensors (Campbell Scientific, Logan, UT). Each plot had paired sensors recording SM at depths of 0–15 cm (shallow) and 15–30 cm (deep) (Figure 1a).

2.2 | Photosynthesis and light

Plants located in each of the microsites indicated in Figure 1, as well as in the control plot, were used to assess differences in light-saturated photosynthesis (A_{sat}) and the quantum yield of CO_2 assimilation (ϕCO_2) in *B. inermis*. Duplicate measurements were made on separate leaves across transects (3 transects, 2 reps, $n = 6$ leaves per microsite). Light responses of leaf-level photosynthesis were measured biweekly during peak growing season (June & July) using a portable photosynthesis system (LI-6800, LI-COR, Inc., Lincoln NE, USA). The LI-6800 was fitted with a 3 × 3 cm cuvette head and a red-blue LED light source. For all measurements, flow rate was held constant at 600 μmol s^{-1}. The LI-6800 temperature exchanger was set to the prevailing midday temperature, which resulted in an average leaf temperature (T_{leaf}) setting of 31.3 ± 2.1°C (standard deviation) across all measurements. Chamber reference CO_2 was set to 420 μmol mol^{-1}, and PPFD was set to 1800 μmol m^{-2} s^{-1} before leaves were placed into the chamber. Once placed in the chamber, leaves typically reached steady state within 5–10 min, at which time a light response curve was initiated.

All measurements occurred between 09:00 and 13:00 local time and were made on recently matured, fully expanded, upper canopy leaves. One-sided surface area of leaves within the chamber was estimated by measuring leaf length and width. Light response curves were constructed by measuring *A* at 12 reference [PPFD] values between 2000 and 0 μmol m^{-2} s^{-1} in a descending stepwise fashion (Figure S1). Each light response curve was parameterized using a non-rectangular parabola (Marshall & Biscoe, 1980) through least squared parameter estimation in R version 4.1.2 (R Core Team, 2017). The model was fit using the *photosynthesis* package (Stinziano et al., 2021) to estimate light-saturated net CO_2 assimilation rate (A_{net}), quantum yield of CO_2 assimilation (ϕCO_2), and light compensation point (LCP, light level needed for photosynthesis to exceed respiration).

2.3 | CO_2 response of photosynthesis

Similar to light response curves, CO_2 response curves of photosynthesis (A-C_i) were measured biweekly during peak growing season (June and July) using a LI-6800. Duplicate measurements were made on separate leaves across transects ($n = 6$ leaves per microsite). Environmental conditions, leaf position, and timing of A-C_i measurements were the same as light response measurements. All A-C_i curves were constructed by measuring net photosynthesis (A_{net}) at 12 reference [CO_2] values between 0 and 1500 μmol mol^{-1} in a stepwise fashion (420, 300, 250, 150, 100, 50, 0, 420, 650, 800, 1200, 1500, see Figure S2). At each reference value, an auto-matching program limited fluctuations of reference CO_2 < 0.1 μmol mol^{-1} before logging to ensure accurate measurements. Each A-C_i curve was parameterized using the Farquhar model of C_3 photosynthesis (Farquhar et al., 1980) using nonlinear least squared parameter estimation in R version 4.1.2 (R Core Team, 2017). The model was fit using the *fitaci* function from the *Plantecophys* package (Duursma, 2015). The model estimates the maximum rate of rubisco carboxylation (V_{cmax}) and the maximum rate of electron transport for RuBP regeneration (J_{max}). The temperature correction function was set to field measurements of T_{leaf} (leaf temperature). Leaf mesophyll conductance to CO_2 was not estimated; thus, V_{cmax} and J_{max} are apparent values that reflect both biochemical limitations and mesophyll conductance (e.g., Salmon et al., 2020). Spot measurements were selected at chamber PPFD 1800 μmol m^{-2} s^{-1} (i.e., saturating light) and reference CO_2 420 μmol mol^{-1} (i.e., ambient CO_2 concentration) to determine relationship between A and g_s. Because a strong relationship between the two was evident (see results), we used measurements of g_s to infer responses in A.

2.4 | Daily plant water relations

At 2-week intervals, daily measurements of stomatal conductance (g_{sw}) were made at five times throughout the day (09:00, 11:00, 13:00, 15:00, and 17:00 h) using a portable porometer/fluorometer (LI-600, LI-COR, Inc., Lincoln NE, USA). Three replicate measurements were taken per experimental plot (between, E_{edge}, beneath, W_{edge}, and control) per transect, resulting in nine replicates across transects ($n = 9$ leaves per microsite). Grass g_{sw} has been shown to be variable along leaf blades (Ocheltree et al., 2012), so as a precautionary measure, all g_{sw} measurements were taken from a standardized point on *B. inermis* leaves.

Leaf water potential (ψ_L) was measured at a similar temporal and spatial frequency throughout the day. Three leaves were removed per plot per transect, resulting in nine plot level replicates. Sampled leaves were placed in plastic bags with damp paper towel. ψ_L was measured on site at JSG using a Scholander-type pressure chamber (PMS Instruments, Corvallis, OR, USA). All leaves were sampled within 40 min of set timepoints, and all measurements were made within an hour.

2.5 | Data analysis

Spatial patterns of ANPP were similar across all transects, so data were analyzed using a one-way analysis of variance (ANOVA) to test plot level effects. Similarly, sunlight (PPFD) and growing season means of daily physiological response (g_{sw} and ψ_L) had little variation at the transect level and as a result were analyzed using one-way ANOVA. Two-way ANOVA was used to test for differences between SM at two measurement depths (0–15 and 15–30 cm) (Microsite × Depth)

and to test how the presence of shade related to daily physiological response (g_{sw} × Shade) and (ψ_L × Shade). A relative weight analysis (RWA package in *R*, cran.r-project.org/web/packages/rwa/rwa.pdf) was used to quantify microsite-level differences of direction and magnitude for total variance in a regression model for g_{sw} and ψ_L into weights, reflecting the proportional contribution of the predictor variables (SM and VPD). RWA allowed us to quantify the proportional influence of covarying environmental drivers on plant physiological processes. Analysis of covariance (ANCOVA) was then used to determine sensitivity of g_{sw} and ψ_L to SM and VPD via microsite-level differences of slope coefficients.

3 | RESULTS

3.1 | Precipitation and temperature

In 2022, annual precipitation at the site was 11% higher than the long-term average (404 vs. 367 mm, respectively). However, the early growing season (April, May, June) was ~40% drier than normal (89 mm in 2022 vs. 148 mm average), and the late growing season (July, August) was ~30% wetter than the long-term average (96 vs. 65 mm, Colorado Climate Center; http://ccc.atmos.colostate.edu/). Mean annual temperature (10.2°C) was slightly above the 30-year average (9.8°C).

3.2 | Light

Compared to open field conditions, light within the array was reduced by ~38.3% during the growing season averaged across all microsites (Figure 2a,b). As expected, plants *Between* rows of panels received the most sunlight within the PV array (72.3% of control), followed by E_{edge} (52%), W_{edge} (37%), and *Beneath* panel (28%). Differences between PPFD on a single cloudless day (Figure 2a,b insets) and means over the growing season highlight the reduced magnitude of afternoon sunlight available to W_{edge} and *Beneath* panel microsites by ~10% and ~6%, respectively. Reduced W_{edge} PPFD in the afternoon was likely a result of increased cloud cover that consistently developed over nearby mountains.

3.3 | SM

Measurements of SM revealed that E_{edge} and W_{edge} microsites were, on average, wetter than all experimental microsites at depths of 0–15 cm (Figure 2, Figure S3). The amplification of precipitation events at panel edges increased shallow SM ~2–4 times more for E_{edge} and W_{edge} compared to controls (Figure 2c,d). Statistically significant differences between shallow and deep SM were only apparent in PV microsites where rainfall was concentrated (W_{edge} and E_{edge}) or impeded (*Beneath*), see Figure 2 and Figure S3. At these microsites, deep soils were typically wetter than shallow, apart from E_{edge} where shallow soils were consistently wetter than deep (Figure 2f, Figure S3). The *Beneath* microsite was relatively unaffected by rainfall events (e.g., did not increase in direct response to precipitation events) yet maintained seasonally consistent moisture status likely through a combination of belowground hydrological processes, lateral moisture transfer from adjacent areas, and reduced evapotranspiration.

3.4 | Plant aboveground productivity

Although a few species other than *B. inermis* persist at the study site, none were present in PV sampling transects, and because of this, ANPP statistical analyses represent *B. inermis* production. Patterns of ANPP were consistent across transects; however, results of a one-way-ANOVA indicated there were statistically significant differences between microsites ($p < 0.001$, Figure 1b). We found that plants in the E_{edge} microsite were on average 30% (±5% SE) more productive ($p < 0.01$) than control, while *Beneath* plants were 22% (±4% SE) less productive than controls. To infer how these results might scale to the landscape level, we standardized ANPP by plot area (following Kannenberg et al., 2023). Averaged across plots and standardized by microsite area, we estimated that ANPP within the array overall was not statistically different from control ANPP ($p = 0.28$), although the calculated mean ANPP in the array was ~6.1% lower than the control.

3.5 | Photosynthetic capacity

On average, we found that A_{sat} and ϕCO_2 were significantly ($p < 0.05$, see Figure 3) higher for plants within the PV array (18.1 ± 1.02 SE, 0.056 ± 0.002 SE, respectively), compared to control plants outside the array (9.7 ± 1.4 SE, 0.038 ± 0.003 SE, respectively). Although differences in V_{cmax}, and J_{max} were not statistically different between PV microsites and control ($p = 0.24$ and 0.11, respectively), means of V_{cmax} and J_{max} were ~32% and 40% higher, respectively (See Figure S4). The strong relationship between *A* and g_s (Figure 3c) at an ambient concentration of CO_2 indicates that measurements of g_{sw} can reliably be inferred as reflective of responses in *A*.

3.6 | Daily water relations patterns

Differences in g_{sw} and ψ_L varied throughout the daily cycle, but temporal differences in these traits depended upon spatial, microsite-level differences (significant Time of Day × Microsite interactions).

3.7 | Stomatal conductance

Based on seasonally averaged daily patterns, E_{edge} plants had significantly higher g_{sw} than plants located in all other experimental microsites ($p < 0.001$) at the first measurement period (9:00 a.m. local

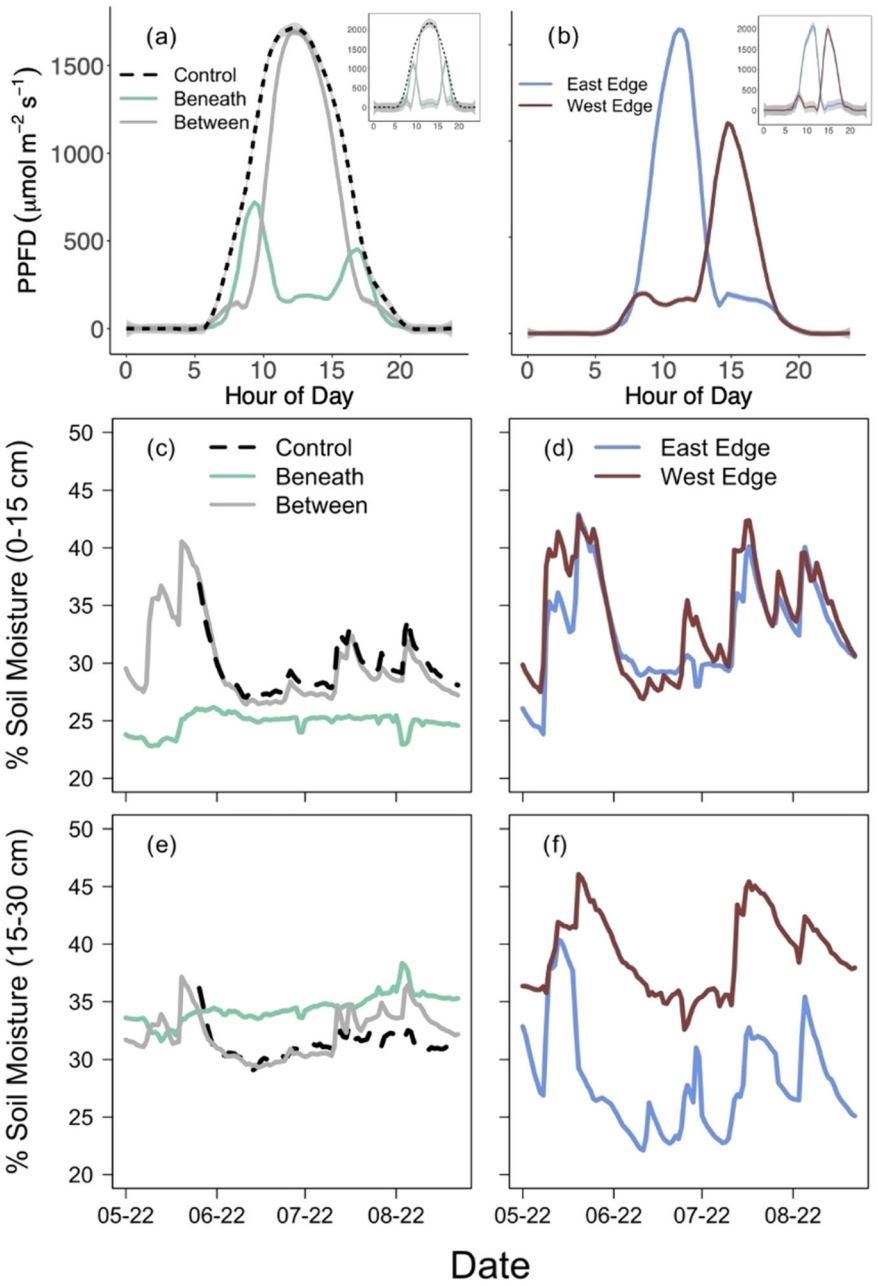


FIGURE 2 (a) Mean growing season patterns of daily photosynthetic photon flux density (PPFD) in a control site (with no influence of the solar array) and in the two solar array microsites that differed dramatically in incident solar radiation (directly beneath and in-between panels). (b) PPFD patterns in two solar array microsites that experience opposing daily patterns of PPFD (morning vs. afternoon sun) as well as unequal amounts of precipitation due to redistribution (runoff) of precipitation occurring primarily in the afternoon from late day thunderstorms. Insets in both (a) and (b) show daily patterns of PPFD on a cloudless day. Gray shadowing on lines representing standard error from the mean. In (c–f), growing season SM is similarly shown, illustrating the concentration of precipitation at panel edges. Note the differences between 0 and 15 cm (c and d) and 15–30 cm (e and f). Plot level statistical differences between shallow and deep SM are shown in Figure S3.

time). This pattern continued throughout the morning (11:00 a.m.), when g_{sw} for E_{edge} and *Beneath* plants were significantly higher than all other plants (Figure 4a). By midday (13:00 p.m.) control plants had significantly lower g_{sw} compared to all plants located within the PV array, and this trend was sustained for much of the day.

To determine how variation among microsite-level daily measurements differed throughout the growing season, a one-way ANOVA was used to compare daily averages of g_{sw} between microsites. The results of this analysis show that E_{edge} had significantly higher ($p = 0.02$) g_{sw} than all other PV (+18%–45%) and control plots (+115%) (Figure 4b). Additional one-way ANOVAs were used to determine how the presence of shade altered microsite-specific response of g_{sw} throughout the growing season. Only experimental microsites in the array were used for this analysis because control plots never experienced PV shade. As expected, the presence of shade significantly reduced g_{sw} across all microsites except for W_{edge}, where plants had 18% ± 4% higher g_{sw} in the shade (Figure 4b inset).

3.8 | Water potential

At the first daily measurement period, plants located in W_{edge} and *Between* microsites had significantly ($p < 0.001$) higher ψ_L than those located in *Control* and *Beneath* microsites. Midmorning measurements at 11:00 a.m. indicated that E_{edge} plants had significantly lower ψ_L than those located in W_{edge} and *Beneath*; however, by midday (13:00 p.m.), microsite-level differences in ψ_L were no longer statistically different. However, in the early afternoon (15:00 p.m.), *Control*

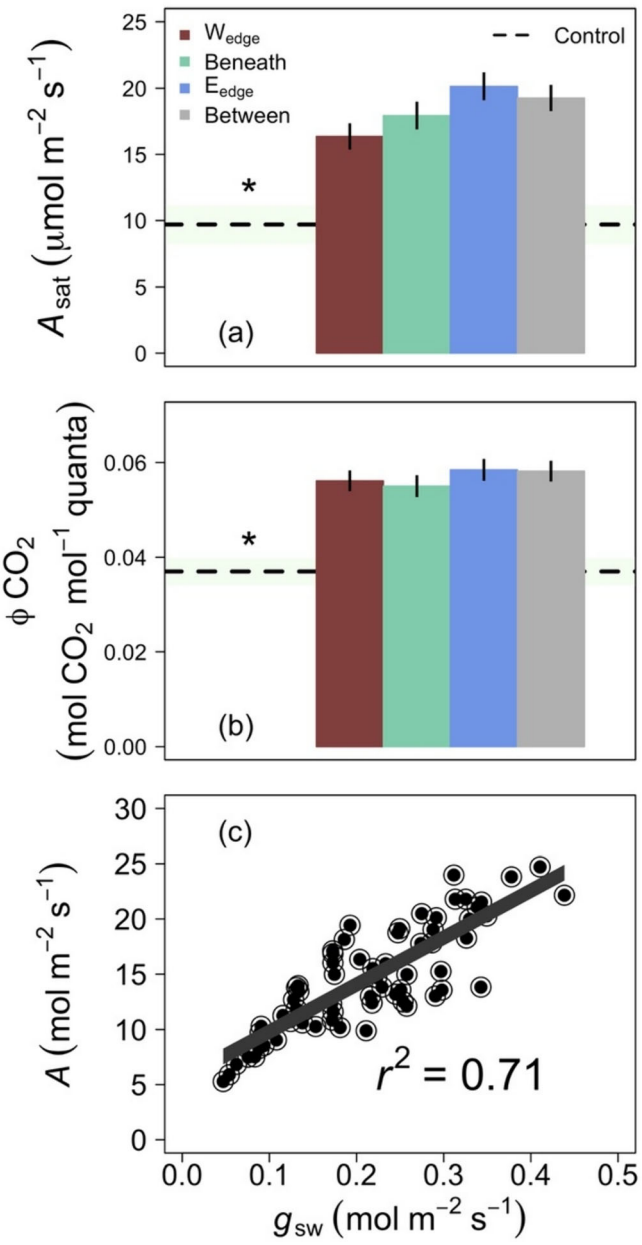


FIGURE 3 Light-saturated photosynthesis (A_{sat}, see panel (a)) and quantum yield of CO_2 assimilation (Φ CO_2, see panel (b)). Solar array microsite means are shown using vertical bars with vertical lines indicating standard error from the mean. The control microsite mean is depicted by a dashed horizontal line with a light green shadow representing standard error from the mean. Star indicates significant difference between control microsite and all solar array microsites (* < 0.05). Relationship between A (assimilation of CO_2) and g_{sw} (stomatal conductance to water vapor) combined for plants in all microsites combined is shown in panel (c).

ψ_L decreased significantly below all other microsites (Figure 4c), and by late afternoon, when final daily measurements were taken, ψ_L for *Beneath* and *Control* plants were significantly lower than plants in all other experimental microsites.

Midday ψ_L is often assumed to estimate maximum daily water stress, so to better illustrate variation in measurement means of this key physiological variable, a separate one-way ANOVA (Figure 4d) was used to analyze a subset of measurements at midday (i.e., solar noon, 13:00 p.m.). This analysis revealed that E_{edge} and *Beneath* plants had significantly higher midday ψ_L than W_{edge}, *Between*, and *Control* plants. As with g_{sw} analyses, additional one-way ANOVAs were used to determine how the presence of shade related to daily response of ψ_L (Figure 4d inset). ψ_L was only significantly higher for *Beneath* and *Between* plants when PV shade was present. The large variation of sun and shade ψ_L for *Between* plants is likely a result of early morning shade (09:00 a.m., Figure 4d) delaying stomatal opening and thus ψ_L was more reflective of soil water potential at the site.

3.9 | Relationships between environmental drivers and plant responses

Through RWA, we determined that SM and VPD had substantially different effects on g_{sw} and ψ_L across the growing season and these effects varied in direction and magnitude between plots (Figure S5). For example, SM contributed to most of the variation in g_{sw} for W_{edge} and *Between* plants, but VPD contributed to most of the variation in ψ_L. However, at the E_{edge} VPD was responsible for variation in g_{sw} and SM for ψ_L. *Beneath* physiological responses were equally impacted by SM and VPD, while variations in *Control* plant g_{sw} and ψ_L were both driven by VPD. The relative contribution of variation attributed to VPD in *Control* plants, however, may also be due to the lack of early season SM measurements in control plots (e.g., Figure 2c).

There was a consistently positive relationship between SM and g_{sw} across plots ($r^2 = 0.54$, Figure 5e) but no significant pattern between SM and ψ_L (Figure 5f). In contrast, both g_{sw} and ψ_L displayed negative relationships in response to increased VPD, with the slopes of those relationships differing between microsites (VPD × Microsite interaction, Figure 5, panels (b, d)), indicating that some plots responded more strongly to VPD. Indeed, comparison of E_{edge} and W_{edge} (Figure 5b,d) highlights the control of VPD on plant water status and thus g_{sw} response, despite both microsites experiencing wetter soils and similar amounts of light availability.

Overall, slopes of relationships between ψ_L and VPD were higher for plants in *Control*, W_{edge}, and *Between* microsites, indicating greater sensitivity to VPD throughout the growing season compared to E_{edge} and *Beneath* plants (Figure 5a,b). In contrast, slopes of relationships between g_{sw} and VPD were more negative for E_{edge} and *Between* plants, indicating more sensitivity in stomatal response to increasing VPD (Figure 5c,d).

4 | DISCUSSION

Our goal was to determine how microsites with different environmental conditions within solar PV arrays can alter physiological responses that underly patterns of productivity in a C_3 grass. Consistent with previous work (Sturchio et al., 2022; Sturchio et al., 2024), we found that plants located on the E_{edge} of PV panels, exposed to morning

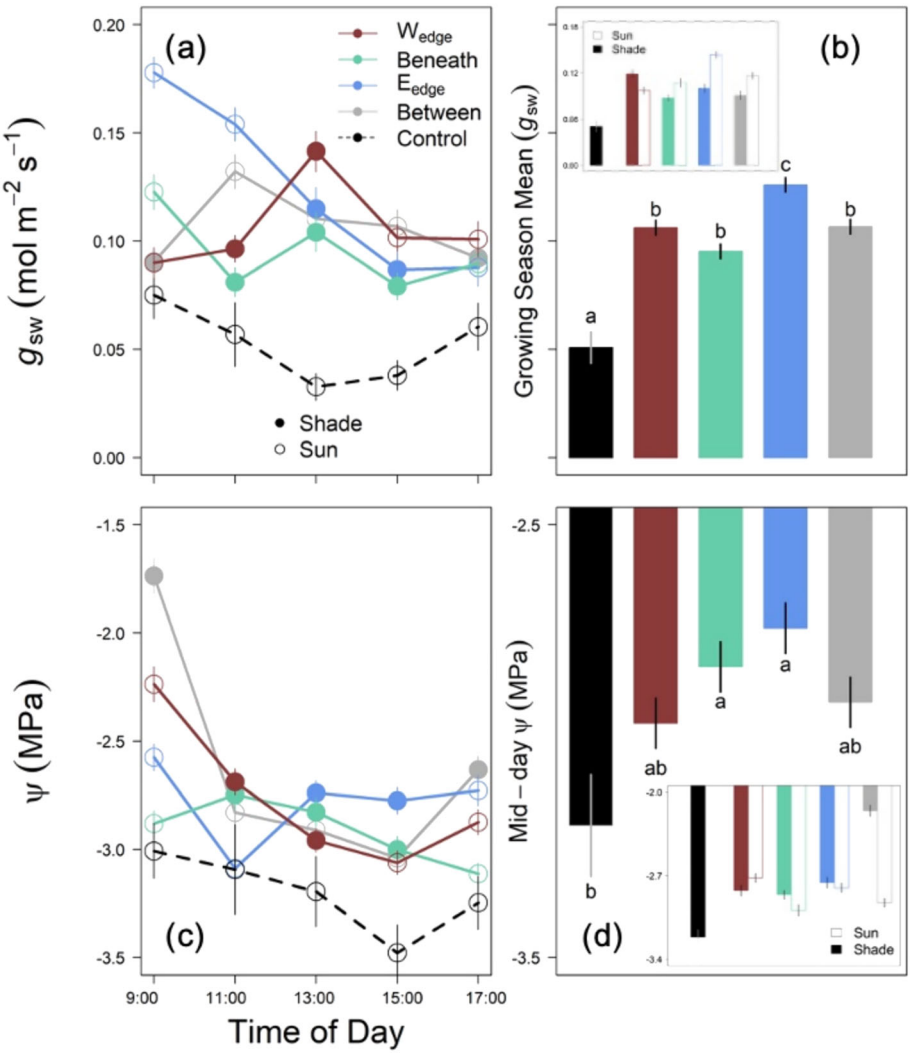


FIGURE 4 Growing season means ($n = 8$ timepoints) of stomatal conductance to water vapor (g_{sw}) and leaf water potential (ψ_L) over time (diurnally, panels (a) and (c)) and across space (microsites, panels (b) and (d)). Open circles indicate timepoints when plants receive direct sunlight, and closed circles indicate when plants are shaded by PV solar panels. Letters above bars represent statistical similarity, where shared letters indicate statistical similarity. Insets in panels (b) and (d) indicate the variable patterns of plant physiology when leaves of different plots experience sun versus shade. In all figure panels, standard error from the mean is depicted with vertical lines.

sunlight and afternoon shade, had the highest ANPP despite receiving less direct sunlight (Figure 2b) than control plants. Surprisingly, photosynthetic parameters (A_{sat}, ϕCO_2) were similar across microsites within the array but were significantly lower for plants growing in control plots outside of the array. These control plants also had consistently lower (leaf water potential) ψ_L throughout the growing season and were presumably more water stressed. We found that plants exposed to primarily morning light consistently had the higher (stomatal conductance to water vapor) g_{sw} and ψ_L throughout the growing season (Figure 4). Additionally, E_{edge} plants had the highest sensitivity of stomatal response to changes in VPD (Figure 5d), but ψ_L was relatively unchanged by changes in VPD (Figure 5b).

4.1 | The importance of the timing of direct sunlight

Strong positive relationships between SM and g_{sw} highlight the importance of SM as a determinant of productivity in water-limited grasslands. However, variation in SM happens at coarser time scales and is less consistent than daily fluctuations of VPD. Daily patterns of g_{sw} and ψ_L are more dependent upon changes in VPD, evidenced by the contrasting relationships between E_{edge} and W_{edge} plants, which receive direct sunlight in the morning or afternoon, respectively (Figure 5a,b). Therefore, SM is likely more physiologically important in PV arrays than previously reported (i.e., Sturchio et al., 2022); however, daily patterns of physiological response indicate that VPD is also important for controlling daily patterns of plant water balance and potentially the apparent differences in end of season production across microsites.

The ability of E_{edge} plants to maintain a consistent ψ_L regardless of changes in VPD is likely due to afternoon shading, reducing physiological stress when atmospheric demand is at its highest. This is in stark contrast to the physiological response of W_{edge} plants that receive a majority of sunlight in the afternoon, where g_{sw} is limited by high VPD (Figure 5d) and ψ_L responds more dynamically (Figure 5c). Although E_{edge} and W_{edge} plants exist just two meters apart and receive nearly identical amounts of direct sunlight daily, the association between time of day and VPD (Figure 6) drastically impacts their diurnal physiology. The relationship between g_{sw} and SM illustrates this point by showing that E_{edge} and W_{edge} plants are capable of similar g_{sw} maximums but that E_{edge} plants achieved those at much lower levels of SM (Figure 5f). However, the relative importance of SM and

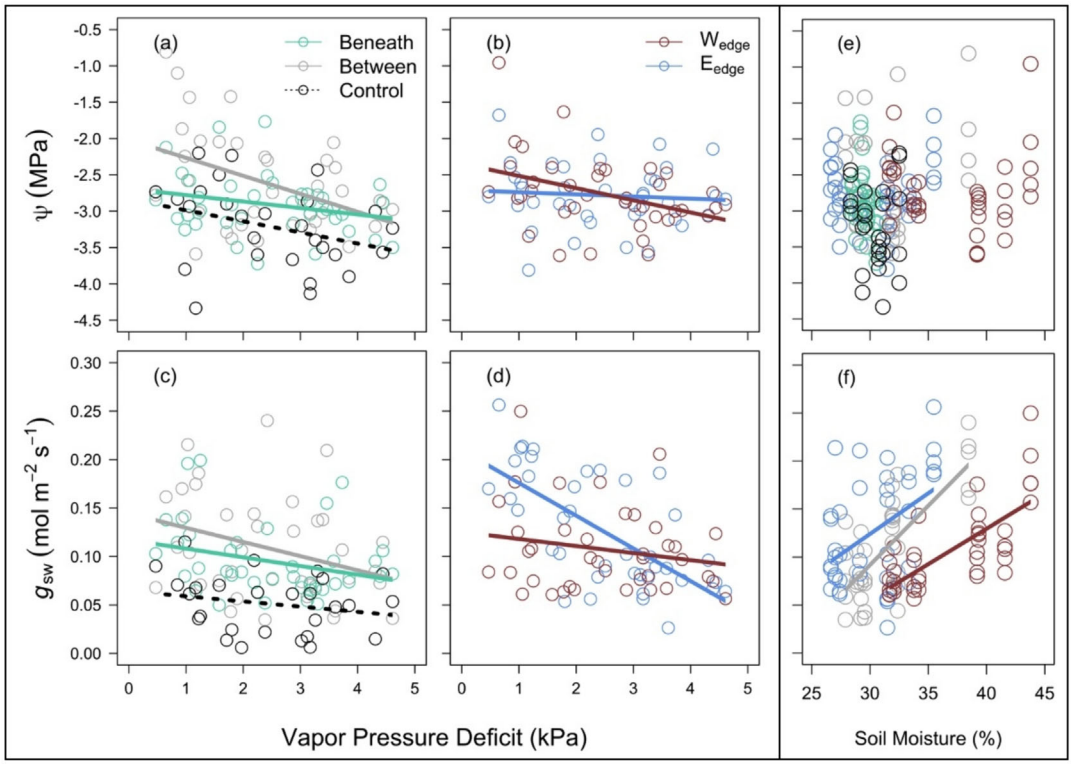


FIGURE 5 Relationships between vapor pressure deficit and leaf physiological traits (panel (c,d): stomatal conductance to water vapor (g_{sw}), $r^2 = 0.36$) and (panel (a,b): leaf water potential (ψ_L), $r^2 = 0.21$) contrasting solar panel induced microsites as in Figure 2. Relationships between soil moisture and leaf physiological traits (e and f) were not split in this way because slopes of relationships were consistent across plots. Note that control and beneath plots are not shown in (f) due to the small range in soil moisture encountered during sampling dates.

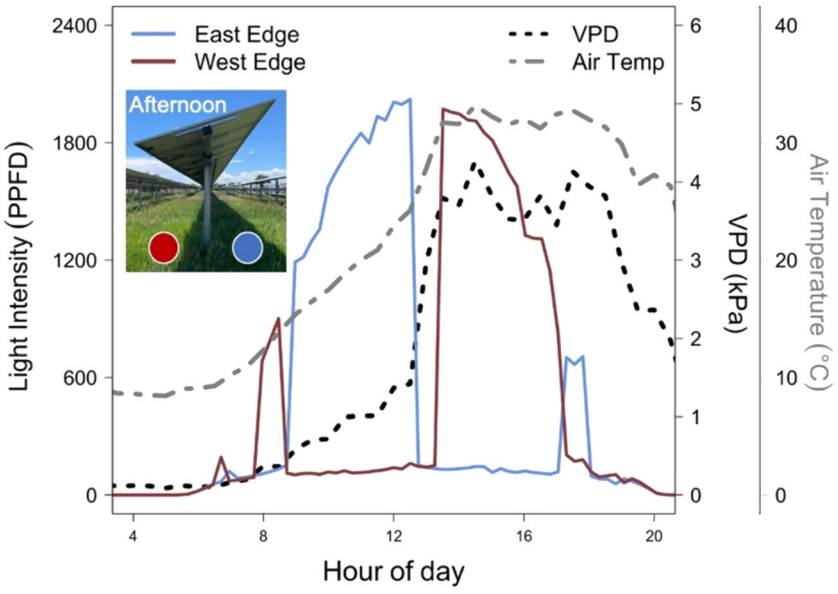


FIGURE 6 Single day example for the daily patterns of environmental drivers of photosynthesis. Red and blue lines indicate light intensity (photosynthetic photon flux density (PPFD)) for plots located identical distance from solar panel support pole on east and west edges, respectively. Dashed black line indicates daily pattern of VPD. Gray line represents air temperature.

VPD as limiting factors of production might be expected to change during drought conditions. Future studies that quantify how these relationships change under severe water limitation will help determine the potential water savings benefits of PV co-location in water-limited ecosystems.

4.2 | Photosynthetic response to novel PV light regimes

Dynamic photosynthetic parameters and their response to alterations in sunlight availability have been well-documented across leaf, plant,

and ecosystem levels (Chazdon & Pearcy, 1991; Emmel et al., 2020; Knapp & Smith, 1990; Kull & Kruijt, 1998; Thornley, 1974). Typically, shade grown leaves acclimate to low light conditions by reducing photosynthetic maxima and light compensation point (i.e., point where photosynthesis exceeds respiration), while increasing the quantum yield of CO_2 assimilation (ϕCO_2) to photosynthesize in low light environments more efficiently (Givnish, 1988; Hamerlynck & Knapp, 1994; Pearcy & Sims, 1994). However, unlike low light conditions found in forest understories, single axis tracking PV arrays allow all plants to consistently receive some extended exposure to full sunlight (Adeh et al., 2018; Sturchio et al., 2022). In this unique environment, we found that despite a ~40% reduction in photosynthetically active light within the array, A_{sat} and ϕCO_2 were both significantly higher for plants inside the PV array compared to control plants (Figure 3). Control plants also had consistently lower midday plant water potential than those within the array. These responses indicate that reductions in the availability of direct sunlight might negligibly impact the overall capacity of photosynthesis in C_3 grasses and a reduction in solar radiation may even help alleviate water stress in dry climates. This finding has important implications for the future design of PV arrays that co-prioritize ecosystem services and energy production (i.e., ecovoltaics, see Sturchio & Knapp, 2023). If light is not a sizeable limitation to photosynthesis in vegetation under the panels, numerous management options could be applied while minimally impacting vegetation carbon uptake and growth.

Temperature is an environmental variable that has demonstrated considerable control on instantaneous and seasonal fluctuations of photosynthetic response (Atkin & Tjoelker, 2003; Smith & Dukes, 2017; Yamori et al., 2014). As previously stated, patterns of stomatal conductance were much different for E_{edge} and W_{edge} plants (morning light vs. afternoon light) (Figures 4, S6); however, these differences had no discernable effect on the photosynthetic response to light and CO_2 (A_{sat}, ϕCO_2, V_{cmax}, and J_{max}, Figures 3, S4) for all plants grown in PV microsites. This result is in contrast to the lower rates of A_{sat} in control plants (Figures 3, S4), which could be the result of a combination of longer exposure to direct sunlight and elevated leaf temperatures (~4°C higher for control plants than PV plants, Figure S7), therefore promoting greater water stress. Temperature response of photosynthesis was not directly tested in this study, but further inquiry may be useful in determining whether biochemical limitation via temperature stress varies between plants grown in PV shade and control plants.

4.3 | Sustainable solar stewardship

As solar land use expands, the economic advantages of solar must also be balanced with the ecological consequences of such development. Forage production is one of the most highly valued ecosystem services provided by rangeland ecosystems (Zhao et al., 2020), and as such, a greater understanding of how PV co-location in grasslands alters forage production dynamics will be important for future management of these dual-use facilities. Our findings highlight the potential importance of daily variation in environmental conditions (temperature and evaporative demand increase throughout the day and reach maximums in afternoon hours) and their respective control of plant productivity. These physiological mechanisms underpinning increases in ANPP illuminate potential synergies for ecovoltaic applications.

Implementation of intentional design and management strategies that utilize PV arrays to facilitate the enhancement of ecosystem services are rare. However, a growing body of research investigating the ecological benefits associated with such an approach can equip landowners, solar developers, and policy makers with the necessary information to make ecologically informed decisions regarding PV development, thus improving the sustainability of PV land use in the long term.

4.4 | Building an ecological understanding of PV ecosystems

As first noted by Smith et al. (1987) more than 30 years ago, in arid and semiarid systems, reductions in solar irradiance from PV panels may be offset by the benefits of higher plant water potential during times of limited water availability. Indeed, the mechanistic importance of *when* light is available might help inform ecologically informed approaches to solar development that prioritize plant water relations over energy production during the hottest and driest days of the growing season (Sturchio & Knapp, 2023). These dynamic PV microenvironments shift the nature of resource limitation in space and time, enabling potential applications related to water stress abatement.

Future work that tests the efficacy of these principles in more diverse grasslands will play an essential role in determining where large-scale solar projects are developed and how they are managed. For example, in more diverse rangelands, there will be more opportunities to assess how plants from different functional groups (i.e., C_3 grass, C_4 grass, forb, shrubs) alter their patterns of physiological response to the unique microenvironmental conditions in an PV array. Of particular interest is determining if C_4 plants (i.e., "warm season" species) respond differently than "cool season" C_3 species to the unique PV-generated microenvironments. Distinct temporal shifts in phenology (Graham et al., 2021) and seasonality (Sturchio et al., 2024) of key ecosystem services (e.g., floral resources and forage quality) have been reported in other PV arrays. A physiologically based investigation for how environmental heterogeneity contributes to phenological patterns of floral production, forage quality, and water use will enable us to better predict ecosystem response and the overall sustainability of PV co-location.

5 | CONCLUSION

In conclusion, we found that microenvironmental conditions created by PV panels altered patterns of photosynthetic response, water

relations, and productivity of a C_3 grass in semiarid Colorado. We report that photosynthetic parameters (A_{sat}, ϕCO_2, V_{cmax}, and J_{max}) were similar for plants in PV microsites but consistently lower in control plants outside the array. This reduction was also present, although muted, in patterns of ANPP, and was likely a result of a combination of higher overall water stress (i.e., coupled response of g_{sw} and ψ_L) and perhaps temperature stress from prolonged exposure to direct sunlight. In fact, the relationship between timing of light availability and atmospheric water demand (i.e., morning vs. afternoon, see Figure 6) limited g_{sw} for plants growing in afternoon sunlight when temperatures were hotter and drier. This work provides mechanistic insight into the physiological processes that underly function in these novel ecosystems. The apparent physiological benefits of shade highlight the compatibility of water-limited grasslands and PV cover, at least for C_3 grasses. Further work that identifies the contribution of environmental conditions to physiological variability across species and biomes is needed to inform sustainable PV co-location.

AUTHOR CONTRIBUTIONS

Matthew A. Sturchio, Steven A. Kannenberg, and Alan K. Knapp conceived and designed the experiment. Matthew A. Sturchio, Steven A. Kannenberg, and Tillie A. Pinkowitz collected the data. Matthew A. Sturchio analyzed the data. Matthew A. Sturchio and Alan K. Knapp wrote the manuscript with input from all authors.

ACKNOWLEDGEMENTS

This work was funded by the US Department of Agriculture's National Institute of Food and Agriculture (NIFA) through the Sustainable Agricultural Systems project entitled "Sustainably Co-locating Agricultural and Photovoltaic Electricity Systems (SCAPES)," led by the University of Illinois Urbana-Champaign, Grant Number: 2021-68012-35898, 2021–2025. The authors would also like to recognize funding from the Stavros Family Fund for Biology research at Colorado State University. Finally, the authors thank Byron Kominek and all of Jack's Solar Garden staff and volunteers for their support and assistance with this experiment.

CONFLICT OF INTEREST STATEMENT

The authors have no conflicts of interest.

DATA AVAILABILITY STATEMENT

The data that support the findings of this study are openly available at https://doi.org/10.5281/zenodo.10447811.

ORCID

Matthew A. Sturchio https://orcid.org/0000-0001-5067-3770
Steven A. Kannenberg https://orcid.org/0000-0002-4097-9140
Alan K. Knapp https://orcid.org/0000-0003-1695-4696

REFERENCES

Adeh, E. H., Selker, J. S., & Higgins, C. W. (2018). Remarkable agrivoltaic influence on soil moisture, micrometeorology and water-use efficiency. *PLoS ONE*, *13*(11), e0203256.

Andrew, A. C., Higgins, C. W., Smallman, M. A., Graham, M., & Ates, S. (2021). Herbage yield, lamb growth and foraging behavior in agrivoltaic production system. *Frontiers in Sustainable Food Systems*, *5*, 659175.

Armstrong, A., Ostle, N. J., & Whitaker, J. (2016). Solar park microclimate and vegetation management effects on grassland carbon cycling. *Environmental Research Letters*, *11*(7), 074016.

Atkin, O. K., & Tjoelker, M. G. (2003). Thermal acclimation and the dynamic response of plant respiration to temperature. *Trends in Plant Science*, *8*(7), 343–351. https://doi.org/10.1016/S1360-1385(03)00136-5

Bai, Z., Jia, A., Bai, Z., Qu, S., Zhang, M., Kong, L., Sun, R., & Wang, M. (2022). Photovoltaic panels have altered grassland plant biodiversity and soil microbial diversity. *Frontiers in Microbiology*, *13*, 1065899.

Barron-Gafford, G. A., Pavao-Zuckerman, M. A., Minor, R. L., Sutter, L. F., Barnett-Moreno, I., Blackett, D. T., Thompson, M., Dimond, K., Gerlak, A. K., Nabhan, G. P., & Macknick, J. E. (2019). Agrivoltaics provide mutual benefits across the food–energy–water nexus in drylands. *Nature Sustainability*, *2*(9), 848–855. https://doi.org/10.1038/s41893-019-0364-5

Cabon, A., Kannenberg, S. A., Arain, A., Babst, F., Baldocchi, D., Belmecheri, S., … Anderegg, W. R. (2022). Cross-biome synthesis of source versus sink limits to tree growth. *Science*, *376*(6594), 758–761.

Chazdon, R. L., & Pearcy, R. W. (1991). The importance of sunflecks for forest understory plants. *BioScience*, *41*(11), 760–766. https://doi.org/10.2307/1311725

Choi, C. S., Cagle, A. E., Macknick, J., Bloom, D. E., Caplan, J. S., & Ravi, S. (2020). Effects of revegetation on soil physical and chemical properties in solar photovoltaic infrastructure. *Frontiers in Environmental Science*, *8*, 140.

Choi, C. S., Macknick, J., Li, Y., Bloom, D., McCall, J., & Ravi, S. (2023). Environmental co-benefits of maintaining native vegetation with solar photovoltaic infrastructure. *Earth's Future*, *11*(6), e2023EF003542.

Dinesh, H., & Pearce, J. M. (2016). The potential of agrivoltaic systems. *Renewable and Sustainable Energy Reviews*, *54*, 299–308.

Dupraz, C., Marrou, H., Talbot, G., Dufour, L., Nogier, A., & Ferard, Y. (2011). Combining solar photovoltaic panels and food crops for optimising land use: Towards new agrivoltaic schemes. *Renewable Energy*, *36*(10), 2725–2732.

Duursma, R. A. (2015). Plantecophys-an R package for analysing and modelling leaf gas exchange data. *PLoS ONE*, *10*(11), e0143346. https://doi.org/10.1371/journal.pone.0143346

Ellsworth, D. S., & Reich, P. B. (1992). Leaf mass per area, nitrogen content and photosynthetic carbon gain in *Acer saccharum* seedlings in contrasting forest light environments. *Functional Ecology*, *6*(4), 423–435.

Emmel, C., D'Odorico, P., Revill, A., Hörtnagl, L., Ammann, C., Buchmann, N., & Eugster, W. (2020). Canopy photosynthesis of six major arable crops is enhanced under diffuse light due to canopy architecture. *Global Change Biology*, *26*(9), 5164–5177.

Farquhar, G. D., von Caemmerer, S. V., & Berry, J. A. (1980). A biochemical model of photosynthetic CO 2 assimilation in leaves of C_3 species. *Planta*, *149*, 78–90.

Feldman, D., Ramasamy, V., Fu, R., Ramdas, A., Desai, J., & Margolis, R. (2021). *US solar photovoltaic system and energy storage cost benchmark (Q1 2020) (No. NREL/TP-6A20-77324)*. National Renewable Energy Lab.(NREL).

Givnish, T. J. (1988). Adaptation to sun and shade: A whole-plant perspective. *Functional Plant Biology*, *15*(2), 63–92. https://doi.org/10.1071/PP9880063

Graham, M., Ates, S., Melathopoulos, A. P., Moldenke, A. R., DeBano, S. J., Best, L. R., & Higgins, C. W. (2021). Partial shading by solar panels delays bloom, increases floral abundance during the late-season for pollinators in a dryland, agrivoltaic ecosystem. *Scientific Reports*, *11*(1), 7452. https://doi.org/10.1038/s41598-021-86756-4

Hamerlynck, E. P., & Knapp, A. K. (1994). Leaf-level responses to light and temperature in two co-occurring Quercus (Fagaceae) species: Implications for tree distribution patterns. *Forest Ecology and Management*, *68*(2–3), 149–159.

Hernandez, R. R., Armstrong, A., Burney, J., Ryan, G., Moore-O'Leary, K., Diédhiou, I., Grodsky, S. M., Saul-Gershenz, L., Davis, R., Macknick, J., Mulvaney, D., Heath, G. A., Easter, S. B., Hoffacker, M. K., Allen, M. F., & Kammen, D. M. (2019). Techno–ecological synergies of solar energy for global sustainability. *Nature Sustainability*, *2*(7), 560–568. https://doi.org/10.1038/s41893-019-0309-z

Hernandez, R. R., Tanner, K. E., Haji, S., Parker, I. M., Pavlik, B. M., & Moore-O'Leary, K. A. (2020). Simulated photovoltaic solar panels alter the seed bank survival of two desert annual plant species. *Plants*, *9*(9), 1125.

Juillion, P., Lopez, G., Fumey, D., Lesniak, V., Génard, M., & Vercambre, G. (2022). Shading apple trees with an agrivoltaic system: Impact on water relations, leaf morphophysiological characteristics and yield determinants. *Scientia Horticulturae*, *306*, 111434.

Kannenberg, S. A., Sturchio, M. A., Venturas, M. D., & Knapp, A. K. (2023). Grassland carbon-water cycling is minimally impacted by a photovoltaic array. *Communications Earth & Environment*, *4*(1), 238.

Knapp, A. K., Fay, P. A., Blair, J. M., Collins, S. L., Smith, M. D., Carlisle, J. D., Harper, C. W., Danner, B. T., Lett, M. S., & McCarron, J. K. (2002). Rainfall variability, carbon cycling, and plant species diversity in a Mesic grassland. *Science*, *298*(5601), 2202–2205. https://doi.org/10.1126/science.1076347

Knapp, A. K., & Smith, W. K. (1990). Stomatal and photosynthetic responses to variable sunlight. *Physiologia Plantarum*, *78*(1), 160–165. https://doi.org/10.1111/j.1399-3054.1990.tb08731.x

Kull, O., & Kruijt, B. (1998). Leaf photosynthetic light response: A mechanistic model for scaling photosynthesis to leaves and canopies. *Functional Ecology*, *12*(5), 767–777.

La Pierre, K. J., Blumenthal, D. M., Brown, C. S., Klein, J. A., & Smith, M. D. (2016). Drivers of variation in aboveground net primary productivity and plant community composition differ across a broad precipitation gradient. *Ecosystems*, *19*, 521–533.

Larson, E. (2020). *Net-zero America: Potential pathways, infrastructure, and impacts*. Princeton University.

Marrou, H., Guilioni, L., Dufour, L., Dupraz, C., & Wery, J. (2013). Microclimate under agrivoltaic systems: Is crop growth rate affected in the partial shade of solar panels? *Agricultural and Forest Meteorology*, *177*, 117–132.

Marshall, B., & Biscoe, P. V. (1980). A model for C3 leaves describing the dependence of net photosynthesis on irradiance. *Journal of Experimental Botany*, *31*(1), 29–39.

Ocheltree, T. W., Nippert, J. B., & Prasad, P. V. V. (2012). Changes in stomatal conductance along grass blades reflect changes in leaf structure. *Plant, Cell & Environment*, *35*(6), 1040–1049.

Pearcy, R. W., & Sims, D. A. (1994). *Photosynthetic acclimation to changing light environments: Scaling from the leaf to the whole plant. Exploitation of environmental heterogeneity by plants. Ecophysiological processes above-and belowground* (pp. 145–174). Academic Press.

Post, A. K., & Knapp, A. K. (2021). How big is big enough? Surprising responses of a semiarid grassland to increasing deluge size. *Global Change Biology*, *27*(6), 1157–1169.

R Core Team. (2017). *R: A language and environment for statistical computing*. R Foundation for Statistical Computing. https://www.R-project.org/

Sala, O. E., Parton, W. J., Joyce, L. A., & Lauenroth, W. K. (1988). Primary production of the central grassland region of the United States. *Ecology*, *69*(1), 40–45.

Salmon, Y., Lintunen, A., Dayet, A., Chan, T., Dewar, R., Vesala, T., & Hölttä, T. (2020). Leaf carbon and water status control stomatal and nonstomatal limitations of photosynthesis in trees. *New Phytologist*, *226*(3), 690–703.

Smith, N. G., & Dukes, J. S. (2013). Plant respiration and photosynthesis in global-scale models: Incorporating acclimation to temperature and CO 2. *Global Change Biology*, *19*(1), 45–63. https://doi.org/10.1111/j.1365-2486.2012.02797.x

Smith, N. G., & Dukes, J. S. (2017). Short-term acclimation to warmer temperatures accelerates leaf carbon exchange processes across plant types. *Global Change Biology*, *23*(11), 4840–4853.

Smith, S. D., Patten, D. T., & Monson, R. K. (1987). Effects of artificially imposed shade on a Sonoran Desert ecosystem: Microclimate and vegetation. *Journal of Arid Environments*, *13*(1), 65.

Stinziano, J. R., Roback, C., Sargent, D., Murphy, B. K., Hudson, P. J., & Muir, C. D. (2021). Principles of resilient coding for plant ecophysiologists. *AoB Plants*, *13*(5), plab059.

Sturchio, M. A., Kannenberg, S. A., & Knapp, A. K. (2024). Agrivoltaic arrays can maintain semi-arid grassland productivity and extend the seasonality of forage quality. *Applied Energy*, *356*, 122418. https://doi.org/10.1016/j.apenergy.2023.122418

Sturchio, M. A., & Knapp, A. K. (2023). Ecovoltaic principles for a more sustainable, ecologically informed solar energy future. *Nature Ecology & Evolution*, *7*, 1746–1749. https://doi.org/10.1038/s41559-023-02174-x

Sturchio, M. A., Macknick, J. E., Barron-Gafford, G. A., Chen, A., Alderfer, C., Condon, K., Hajek, O. L., Miller, B., Pauletto, B., Siggers, J. A., Slette, I. J., & Knapp, A. K. (2022). Grassland productivity responds unexpectedly to dynamic light and soil water environments induced by photovoltaic arrays. *Ecosphere*, *13*(12), e4334.

Tanner, K. E., Moore-O'Leary, K. A., Parker, I. M., Pavlik, B. M., Haji, S., & Hernandez, R. R. (2021). Microhabitats associated with solar energy development alter demography of two desert annuals. *Ecological Applications*, *31*(6), e02349. https://doi.org/10.1002/eap.2349

Tanner, K. E., Moore-O'Leary, K. A., Parker, I. M., Pavlik, B. M., & Hernandez, R. R. (2020). Simulated solar panels create altered microhabitats in desert landforms. *Ecosphere*, *11*(4), e03089.

Thornley, J. H. M. (1974). Light fluctuations and photosynthesis. *Annals of Botany*, *38*(2), 363–373.

Wright, I. J., Reich, P. B., Westoby, M., Ackerly, D. D., Baruch, Z., Bongers, F., … Villar, R. (2004). The worldwide leaf economics spectrum. *Nature*, *428*(6985), 821–827.

Wynne-Sison, T., Devitt, D. A., & Smith, S. D. (2023). Ecovoltaics: Maintaining native plants and wash connectivity inside a Mojave Desert solar facility leads to favorable growing conditions. *Landscape*, *12*(10), 1950.

Yamori, W., Hikosaka, K., & Way, D. A. (2014). Temperature response of photosynthesis in C3, C4, and CAM plants: Temperature acclimation and temperature adaptation. *Photosynthesis Research*, *119*, 101–117.

Zhang, B., Zhang, R., Li, Y., Wang, S., Zhang, M., & Xing, F. (2024). Deploying photovoltaic arrays in degraded grasslands is a promising win-win strategy for promoting grassland restoration and resolving land use conflicts. *Journal of Environmental Management*, *349*, 119495.

Zhao, Y., Liu, Z., & Wu, J. (2020). Grassland ecosystem services: A systematic review of research advances and future directions. *Landscape Ecology*, *35*, 793–814.

SUPPORTING INFORMATION

Additional supporting information can be found online in the Supporting Information section at the end of this article.

How to cite this article: Sturchio, M. A., Kannenberg, S. A., Pinkowitz, T. A., & Knapp, A. K. (2024). Solar arrays create novel environments that uniquely alter plant responses. *Plants, People, Planet*, *6*(6), 1522–1533. https://doi.org/10.1002/ppp3.10554